

NAVAL POSTGRADUATE SCHOOL

Monterey, California



THESIS

**GEOACOUSTIC INVERSION USING DIRECT METHODS
ON AMBIENT NOISE AND EXPLOSIVE ACOUSTIC DATA
IN A SHALLOW WATER WAVEGUIDE**

by

José G. Rojas

March 1998

Thesis Advisor:
Second Reader:

Kevin B. Smith
James V. Sanders

Approved for public release; distribution is unlimited.

DTIC QUALITY INSPECTED 2

19980514 075

REPORT DOCUMENTATION PAGE			Form Approved No. 0704-0188		OMB
Public reporting burden for this collection of information is estimated to average 1 hour per response, including the time for reviewing instructions, searching existing data sources, gathering and maintaining the data needed, and completing and reviewing the collection of information. Send comments regarding this burden estimate or any other aspect of this collection of information suggestions for reducing this burden to Washington Headquarters Services, Directorate for Information Operations and Reports, 1215 Jefferson Davis Highway, Suite 1204, Arlington, VA 22202-4302, and to the Office of Management and Budget, Paperwork Reduction Project (0704-0188), Washington, DC 20503.					
1. AGENCY USE ONLY (Leave Blank)		2. REPORT DATE March 1998		3. REPORT TYPE AND DATES COVERED Master's Thesis	
4. TITLE AND SUBTITLE GEOACOUSTIC INVERSION USING DIRECT METHODS ON AMBIENT NOISE AND EXPLOSIVE ACOUSTIC DATA IN A SHALLOW WATER WAVEGUIDE				5. FUNDING NUMBERS	
6. AUTHOR(S) Rojas, Jose G.					
7. PERFORMING ORGANIZATION NAME(S) AND ADDRESS(ES) Naval Postgraduate School Monterey, CA 93943-5000				8. PERFORMING ORGANIZATION REPORT NUMBER	
9. SPONSORING/MONITORING AGENCY NAME(S) AND ADDRESS(ES)				10. SPONSORING/MONITORING AGENCY REPORT NUMBER	
11. SUPPLEMENTARY NOTES The views expressed in this thesis are those of the author and do not reflect the official policy or position of the Department of Defense or the U.S. Government.					
12a. DISTRIBUTION/AVAILABILITY STATEMENT Approved for public release; distribution is unlimited.				12b. DISTRIBUTION CODE	
13. ABSTRACT (maximum 200 words) The fundamental goal of this thesis is to determine the geoacoustic parameters of a shallow water seabed using direct analysis methods on ambient noise and broadband explosive acoustic data. All data considered are from the Mid-Atlantic Bight shelf break experiment that was conducted from 19 July to 9 August 1996. Simple, theoretical treatments of acoustic propagation in a shallow-water waveguide are applied to specific, measurable quantities in the data which can be inverted directly to produce estimates of bottom compressional sound speed, density, and attenuation. Shear influences are neglected throughout. Specifically, vertical coherence of the ambient noise is used to determine the sound speed contrast at the water/bottom interface, mode travel times extracted from spectrograms of explosive data are used to estimate bottom density based on the concept of an ideal waveguide effective depth, and mode attenuation as a function of range extracted from similar spectrograms are employed to estimate attenuation. These direct inversion methods are less accurate than sophisticated matched field processing techniques or direct core measurements, but they do provide a relatively simple means of obtaining reasonable estimates of ocean bottom parameters from minimal information.					
14. SUBJECT TERMS geoacoustic inversion				15. NUMBER OF PAGES 43	
				16. PRICE CODE	
17. SECURITY CLASSIFICATION OF REPORT Unclassified	18. SECURITY CLASSIFICATION OF THIS PAGE Unclassified	19. SECURITY CLASSIFICATION OF ABSTRACT Unclassified	20. LIMITATION OF ABSTRACT UL		

Approved for public release; distribution is unlimited.

**GEOACOUSTIC INVERSION USING DIRECT METHODS ON AMBIENT NOISE
AND EXPLOSIVE ACOUSTIC DATA IN A SHALLOW WATER WAVEGUIDE**

José G. Rojas
Commander, Venezuelan Navy
B.S., Venezuelan Naval Academy, 1981

Submitted in partial fulfillment
of the requirements for the degree of


MASTER OF SCIENCE IN ENGINEERING ACOUSTICS

from the

NAVAL POSTGRADUATE SCHOOL

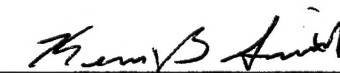
March 1998

Author:

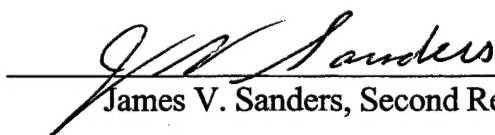


José G. Rojas

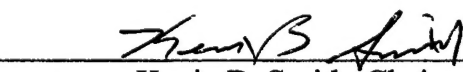
Approved by:



Kevin B. Smith, Thesis Advisor



James V. Sanders, Second Reader



Kevin B. Smith, Chairman
Engineering Acoustics Academic Committee

ABSTRACT

The fundamental goal of this thesis is to determine the geoacoustic parameters of a shallow water seabed using direct analysis methods on ambient noise and broadband explosive acoustic data. All data considered are from the Mid-Atlantic Bight shelf break experiment that was conducted from 19 July to 9 August 1996. Simple, theoretical treatments of acoustic propagation in a shallow-water waveguide are applied to specific, measurable quantities in the data which can be inverted directly to produce estimates of bottom compressional sound speed, density, and attenuation. Shear influences are neglected throughout. Specifically, vertical coherence of the ambient noise is used to determine the sound speed contrast at the water/bottom interface, mode travel times extracted from spectrograms of explosive data are used to estimate bottom density based on the concept of an ideal waveguide effective depth, and mode attenuation as a function of range extracted from similar spectrograms are employed to estimate attenuation. These direct inversion methods are less accurate than sophisticated matched field processing techniques or direct core measurements, but they do provide a relatively simple means of obtaining reasonable estimates of ocean bottom parameters from minimal information.

TABLE OF CONTENTS

I.	INTRODUCTION	1
A.	MID-ATLANTIC BIGHT OBJECTIVES	1
B.	STUDY OBJECTIVES	1
II.	EXPERIMENTAL/ENVIRONMENTAL DESCRIPTION	3
III.	ANALYSIS METHODS	7
A.	INVERSION OF BOTTOM SOUND SPEED	7
B.	INVERSION OF BOTTOM DENSITY	10
C.	INVERSION OF BOTTOM ATTENUATION	14
IV.	DATA ANALYSIS AND RESULTS	19
A.	INVERSION OF BOTTOM SOUND SPEED	19
B.	INVERSION OF BOTTOM DENSITY	20
C.	INVERSION OF BOTTOM ATTENUATION	21
V.	CONCLUSION	25
	LIST OF REFERENCES	27
	INITIAL DISTRIBUTION LIST	29

LIST OF FIGURES

1.	Arrangement and Location of Acoustic Elements Used at the Experimental Site....	4
2.	Sound Speed Profile Measured Near the Trial Site and Used in This Study	5
3.	Example of Ideal Vertical Coherence Function Versus Frequency.....	8
4.	Model of the Vertical Distribution of Ambient Noise in a Pekeris Waveguide.....	9
5.	Geometry Used to Derive the Effective Boundary Depth.	11
6.	Geometry Used to Find the Number of Bottom Bounces.....	15
7.	Coherence of the Measured Ambient Noise Between Two Hydrophones; Real Component (Dashed Curve) and Imaginary Component (Dotted Curve). A Good Fit Between the Theoretical Coherence Obtained from the Model (Solid Line) and the Real of the Measured Coherence is Observed.....	22
8.	Ambiguity Surface for the Optimization with Two Parameters, a_2 and θ_c . The Minimum is Marked by X Which Corresponds to $a_2 \approx 0.18$ and $\theta_c \approx 18^\circ$ for 4 Different SUS Explosive Data.....	23
9a.	Mode Travel Times for a Phone from a SUS Explosive Data.....	24
9b.	Mode Travel Times for a Phone from an Ideal Waveguide.....	24

ACKNOWLEDGMENT

This thesis has been the most difficult task in my career. However, I recognize that it was an excellent experience in learning about the very interesting and difficult subject of acoustics. Completing this job was possible with the help and generosity of many people. First, I would like to thank my thesis advisor, Professor Kevin B. Smith, for his patience, guidance, knowledge, supervision and instruction during this difficult task. In addition, I want to say that without Kevin's knowledge it would have been too difficult to complete the objectives of this thesis.

I would also like to thank Chris Miller, the Coact lab supervisor, for all of his useful assistance. Chris was always positive in giving me an accurate answer to my questions.

I wish to acknowledge my colleagues of the "Underseawater Acoustics and Oceanography study group": LCDR J. Brune, LT A. Bettega, LT Abrantes, and LT L. Pibernat. They gave me important inputs to complete this work.

My wife, Merkys, I salute not only for her loving familial support, but also for her tireless efforts and interest in learning another language. My daughters Geraldine and Gabriela are as lucky to have her as I am.

Finally, I thank my wonderful mother, whose love, blessing and support give me drive and the need to improve myself.

I. INTRODUCTION

A. MID-ATLANTIC BIGHT OBJECTIVES

Better knowledge of operating environments may allow any Navy to improve the use of its USW systems in different tactical scenarios. Even though undersea sound and its practical uses have been continuously explored since World War II, testing of other techniques are necessary in order to obtain important sea environment information which may help in the development of accurate Naval USW systems. To face this challenge, the Mid-Atlantic Bight (MAB) experiment was conducted. The MAB experiment was an intensive field study of the shelfbreak south of Long Island during the strongly stratified summer season whose basic objectives were:

1. To provide detailed time series of the oceanographic conditions along typical major acoustic paths by using moored acoustical arrays.
2. To provide a diversity of frequencies and source locations from broadband SUS sources.
3. To determine the temperature structure of the ocean environment by using acoustic tomography.

This study may provide the Navy an alternative and simple means of determining characteristics in unknown or poorly known operating environments. (Pickart et al., 1996)

B. STUDY OBJECTIVES

The objectives for reaching the fundamental goal of this study are as follows:

1. To determine the bottom sound speed by measuring the coherence of two vertically displaced sensors in the shallow water channel and comparing this function with one obtained from a simple model equation over a range of frequencies.
2. To determine the bottom density by comparing mode travel times of computed spectrograms for a phone from SUS explosive data and those obtained by employing the concept of an effective depth for an ideal waveguide.

3. To determine the bottom attenuation by finding mode attenuation as a function of range extracted from spectrograms and relating it to loss per bottom bounce.

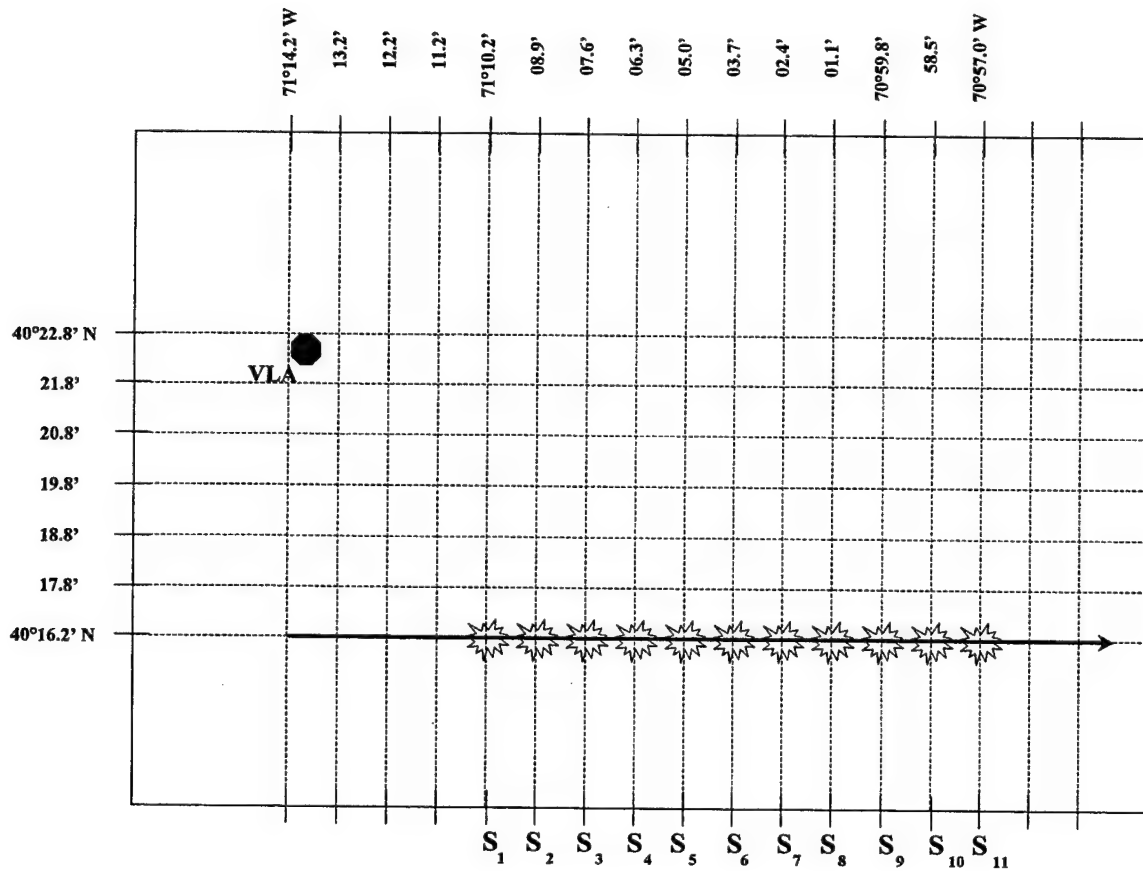
II. EXPERIMENTAL/ENVIRONMENTAL DESCRIPTION

The summer Mid-Atlantic Bight experiment consisted of a cruise from 19 July to 9 August 1996 aboard the R/V Endeavor from the University of Rhode Island. The cruise included three major components: acoustic tomography, SEASOAR operations, and hydrography/tracers. An AXBT flight was also conducted during this time period, as well as a SUS drop fly-over. The acoustic portion of the experiment consisted of three components:

1. The moored acoustic transmission array, or tomography array
2. The moored physical oceanography array, which provided detailed time series of the oceanographic conditions along our major acoustic path
3. The broadband, explosive (MK61 SUS shot) source component.

Multiple lines of SUS drops were deployed in the area by P-3 aircraft and monitored by two vertical line arrays (VLAs) moored on the shelf in ~85m water. (Pickart et al., 1996)

To achieve the objectives of this thesis, eleven broadband SUS shot transmissions recorded at the NW VLA were selected. All of these were dropped along a single track from a point at latitude $40^{\circ}16.2'N$, longitude $71^{\circ}10.2'W$ to a point at latitude $40^{\circ}16.8'N$, longitude $70^{\circ}57.0'W$. The sampling rate was 3906.25 Hz, the duration of one record was 8.3886 sec and the number of samples/record was 32768. The arrangement and the location of the acoustical elements used for this study are shown in Figure 1. This region of the experimental site has a nominal water depth of ~ 90 m with little variation (<10m) from the VLA to the positions of the selected SUS drops. The receiving VLA had 16 hydrophones of which only the upper 8 successfully recorded the SUS transmissions with an upper depth of 30.5 m and inter-element spacing of 3.5m. A typical sound speed profile measured near the trial site and used in this analysis is shown in Figure 2.



Acoustical Element	Latitude	Longitude	Distance to VLA (km)
VLA	40°22.4'	71°13.5'	
SUS-S ₁	40°16.2'	71°10.2'	13.00
SUS-S ₂	40°16.2'	71°08.9'	14.30
SUS-S ₃	40°16.2'	71°07.6'	15.85
SUS-S ₄	40°16.2'	71°06.3'	17.60
SUS-S ₅	40°16.2'	71°05.0'	19.50
SUS-S ₆	40°16.2'	71°03.7'	21.50
SUS-S ₇	40°16.2'	71°02.4'	23.50
SUS-S ₈	40°16.2'	71.01.1'	25.70
SUS-S ₉	40°16.2'	70°59.8'	27.80
SUS-S ₁₀	40°16.2'	70°58.5'	30.00
SUS-S ₁₁	40°16.2'	70°57.0'	32.60

Figure 1. Arrangement and Location of Acoustic Elements Used at the Experimental Site.

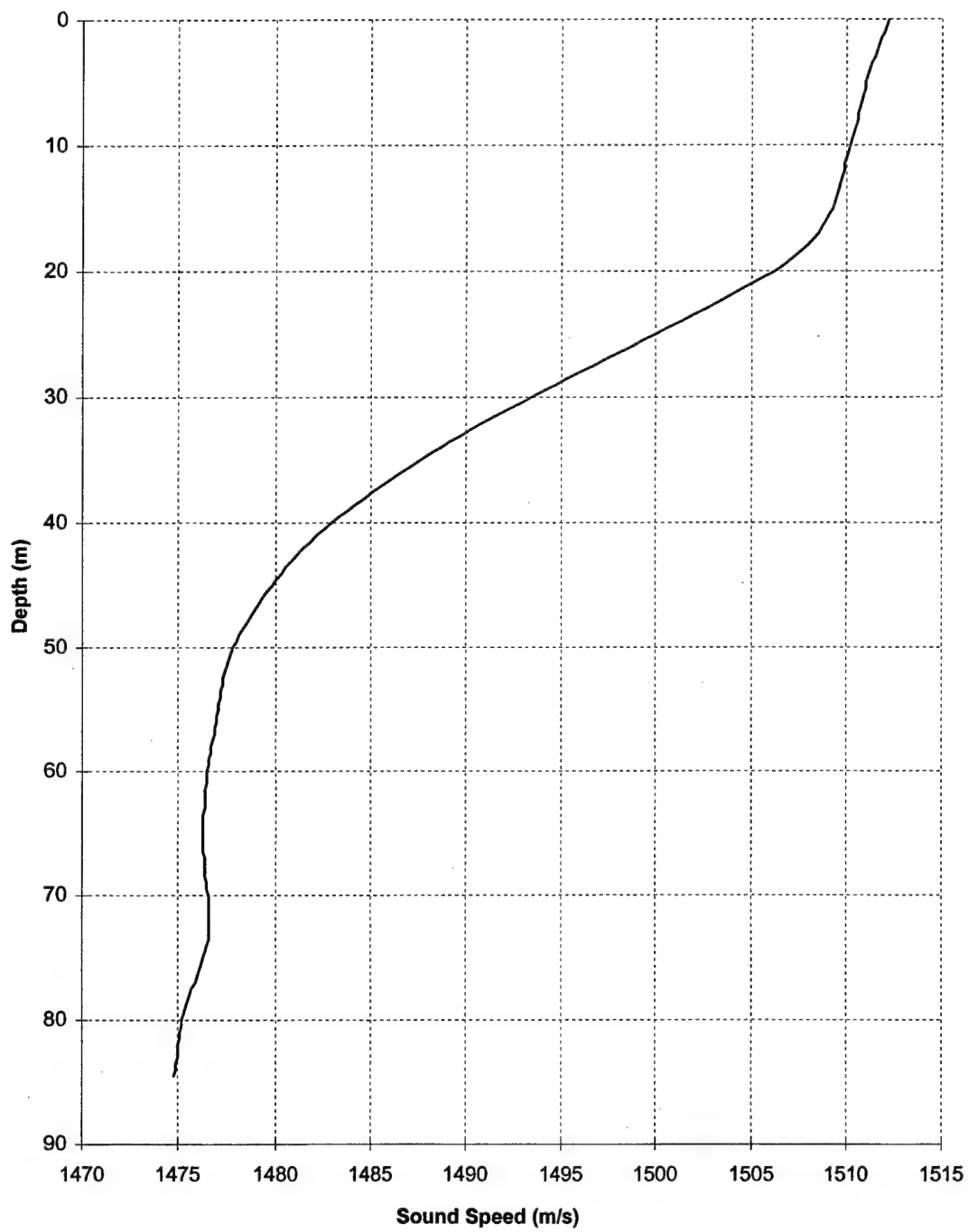


Figure 2. Sound Speed Profile Measured Near the Trial Site and Used in This Study.

III. ANALYSIS METHODS

A. INVERSION OF BOTTOM SOUND SPEED

In determining the bottom sound speed a method was performed to determine the critical angle of the seabed from the vertical directionality of the ambient noise in the water column (Buckingham and Jones, 1987). The properties of the ambient noise that we are specifically concerned with are the vertical directionality and the spatial coherence of the fluctuations of two sensors vertically displaced in the noise field. These two quantities are related through a Fourier transform relationship, which is given by

$$\Gamma(\Omega) = \frac{1}{2} \int_0^\pi F(\theta) \exp[i\Omega \cos(\theta)] \sin(\theta) d\theta \quad (1)$$

where θ is the polar angle measured down from the zenith and $F(\theta)$ is a dimensionless directional density function which represents the distribution of the noise power in the vertical. $F(\theta)$ can be normalized according to the condition

$$\frac{1}{2} \int_0^\pi F(\theta) \sin(\theta) d\theta = 1. \quad (2)$$

This indicates that in the limit as $\Omega \rightarrow 0$ the value of the coherence function goes to unity.

Buckingham and Jones provided a simple example for isotropic noise in which $F(\theta)$ is independent of θ . According to Eqs. (1) and (2) the coherence function in this case is shown to be

$$\Gamma_{\text{isotr}}(\Omega) = \frac{\sin(\Omega)}{\Omega}, \quad (3)$$

where Ω is a dimensionless angular frequency defined as

$$\Omega = \frac{\omega l}{c_w}, \quad (4)$$

ω is the angular frequency, c_w is the sound speed in the water column, and l is the separation between the two sensor positions. This example is shown in Figure 3.

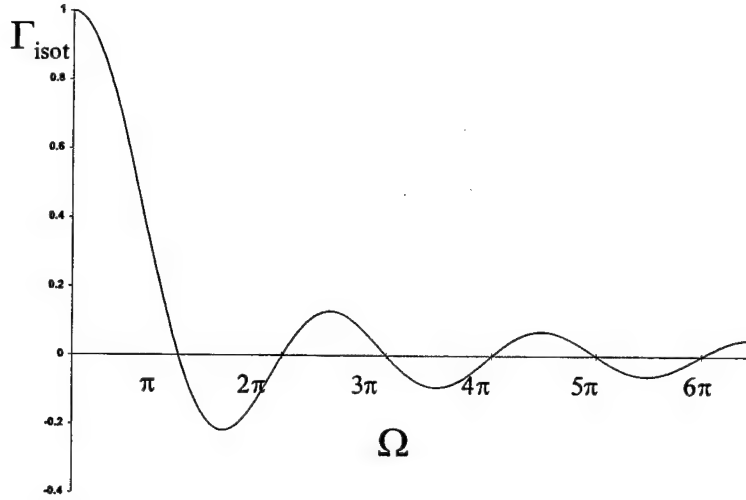


Figure 3. Example of Ideal Vertical Coherence Function Versus Frequency.

This function predicts that the coherence of the noise at two sensors is real due to symmetry of the noise field about the horizontal. For an asymmetrical noise distribution in the vertical, the coherence function is complex with a large imaginary component. A symmetrical noise distribution is also predicted by Buckingham and Jones' theoretical model of shallow water noise, where the coherence function for shallow water noise is an oscillatory function that decays with increasing Ω . At a given frequency, the directional density function of the noise predicted by the model is closely approximated by

$$F_1(\theta) = \begin{cases} a_1, & \text{for } \left(\frac{\pi}{2} - \theta_c\right) \leq \theta \leq \left(\frac{\pi}{2} + \theta_c\right), \\ 0, & \text{otherwise} \end{cases} \quad (5)$$

where a_1 is independent of θ . Then, the noise propagates in directions close to the horizontal, with no acoustic energy traveling with grazing angles greater than θ_c (the critical grazing angle). The contribution of local, wind-driven sources to the overall noise field is approximately isotropic, that is, the directional density function of the continuous component of the noise can be expressed as

$$F_2(\theta) = a_2, \text{ for } 0 \leq \theta \leq \pi, \quad (6)$$

where a_2 is independent of θ . By superposing Eqs. (5) and (6) we have a representative directional density function for the total noise field in shallow water:

$$F_{sw}(\theta) = F_1(\theta) + F_2(\theta) = \begin{cases} (a_1 + a_2), & \text{for } \left(\frac{\pi}{2} - \theta_c\right) \leq \theta \leq \left(\frac{\pi}{2} + \theta_c\right) \\ a_2, & \text{otherwise.} \end{cases} \quad (7)$$

Figure 4 shows a sketch of the vertical distribution expected in a shallow water environment. Through the normalization condition in Eq. (2), the critical grazing angle can be expressed in terms of the other two parameters as

$$\sin(\theta_c) = \frac{1 - a_1}{a_2}, \quad (8)$$

and the model coherence function of the noise represented by the distribution in Eq. (7) is found from Eq. (1) to be

$$\Gamma_{sw}(\theta) = \frac{a_2}{\Omega} \sin(\Omega) + \frac{1 - a_2}{\Omega \sin(\theta_c)} \sin[\Omega \sin(\theta_c)]. \quad (9)$$

Using this model, the spatial coherence of two vertically displaced sensors of the NW VLA was computed from extracted ambient noise data. By spatial coherence is meant

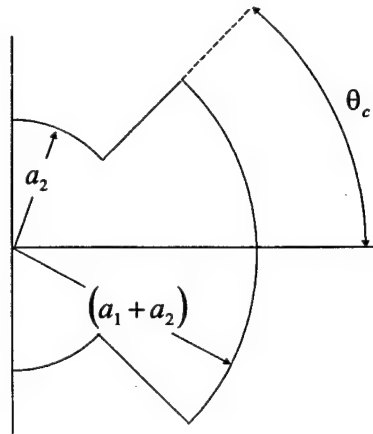


Figure 4. Model of the Vertical Distribution of Ambient Noise in a Pekeris Waveguide.

the time-averaged crosscorrelation coefficient of the noise observed by hydrophones separated vertically in the water column, i.e.,

$$\Gamma_{meas} = \frac{P_{xy}(\omega)}{\sqrt{P_{xx}(\omega)P_{yy}(\omega)}}, \quad (10)$$

where $P_{xy}(\omega)$ represents the cross spectral density as a function of frequency for two separated phones and $P_{xx}(\omega)$ and $P_{yy}(\omega)$ represent the spectral density for each one of the separated phones. To search the two unknown parameters a_2 and θ_c in Eq. (9), an optimization procedure was implemented by finding a least squares fit between the real part of the measured coherence function, Γ_{meas} , and the theoretical coherence function, Γ_{sw} . By defining the ambiguity function

$$\Phi = \sum_{n=1}^N |\Gamma_{sw}(\Omega, a_2, \theta_c) - \text{Real}\{\Gamma_{meas}(\Omega)\}|^2, \quad (11)$$

values for a_2 and θ_c are obtained when Φ is a minimum.

B. INVERSION OF BOTTOM DENSITY

To determine the bottom density, the concept of an effective depth for an ideal waveguide was employed (Chapman and Ward, 1989). By considering the phase change of a plane wave reflected at a fluid/fluid boundary, Weston introduced the concept of the effective boundary depth, arguing that one could view the reflection as taking place at an imaginary pressure - release boundary located at a specific depth below the true boundary. He proposed that the normal modes of the Pekeris model should be similar to those of an ideal pressure - release waveguide whose depth was equal to the true water depth plus the effective boundary depth. The normal mode wavenumbers for the Pekeris model can then be estimated easily without numerical iteration.

The Pekeris model consists of a uniform water layer of constant depth bounded above by a pressure - release surface and below by a uniform fluid half space having different density and sound speed. Consider a plane wave of frequency f in a fluid medium

of sound speed c_w incident upon a plane boundary with another acoustic medium at angle θ relative to grazing, as depicted in Figure 5.

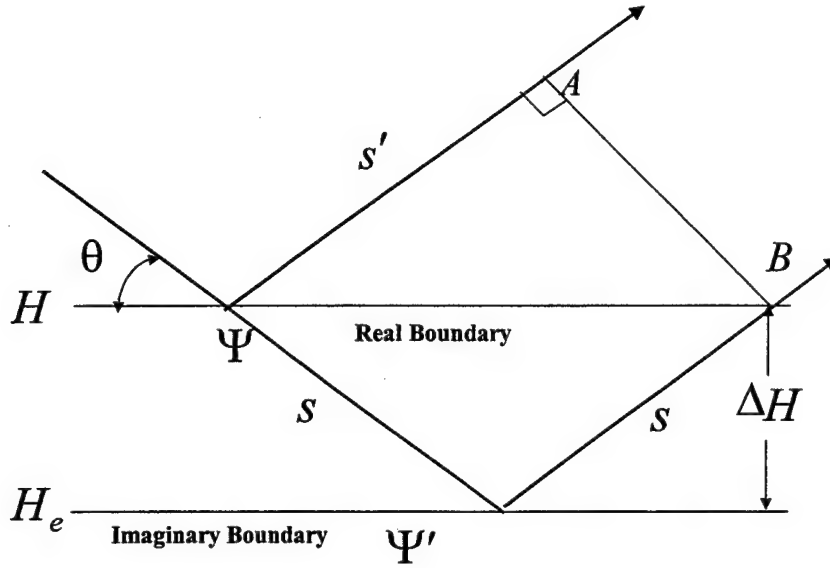


Figure 5. Geometry Used to Derive The Effective Boundary Depth.

The ray segments s and s' are given by

$$s = \frac{\Delta H}{\sin \theta} \quad (12)$$

and

$$s' = \frac{2\Delta H \cos^2 \theta}{\sin \theta}, \quad (13)$$

and the phase of the reflected plane wave at points A and B is given by

$$\phi_A = k_w s' + \Psi \quad (14)$$

and

$$\phi_B = 2k_w s + \Psi', \quad (15)$$

in which $k_w = \frac{\omega}{c_w}$. Requiring $\phi_A = \phi_B$ the effective depth of the boundary is defined by

$$H_e(\theta) - H = \frac{\Psi - \Psi'}{2k_w \sin \theta}. \quad (16)$$

For an isospeed water column with sound speed c_w and density ρ_w overlying a homogeneous solid medium with compressional sound speed c_b , shear speed c_s , and density ρ_b , Chapman and Ward (1984), have shown (assuming $c_s < c_w$ and bottom attenuation is negligible) that the effective depth is

$$H_e = H + \left[1 - 2 \left(\frac{c_s}{c_w} \right)^2 \right] \frac{g}{k_w \sin \theta_c}, \quad (17)$$

where H is the water depth and θ_c is the grazing critical angle. If $c_s \ll c_w$ then Eq. (17) is reduced to

$$H_e = H + \frac{g}{k_w \sin \theta_c}. \quad (18)$$

The boundary conditions for this ideal waveguide require the pressure to vanish at the upper and lower interfaces. Correspondingly, eigenfunctions, $\psi(z)$, must satisfy (Medwin and Clay, 1998)

$$\psi(z)|_{z=0} = 0 \text{ and } \psi(z)|_{z=H_e} = 0. \quad (19)$$

Solutions of the eigenfunctions for these boundary conditions are

$$\psi(z) = \sin \left(\frac{n\pi z}{H_e} \right), \quad (20)$$

and the vertical component of the wavenumber, γ , must then satisfy the quantization condition

$$\gamma_n = \frac{n\pi}{H_e}, \quad (21)$$

where n is the integer and designates the mode number. The horizontal values of the wavenumber K_n are then given by

$$K_n = (k_w^2 - \gamma_n^2)^{1/2}, \quad (22)$$

and the requirement that K_n be real gives the mode cut-off. By substituting γ_n from Eq.

(21) and $k_w = \frac{\omega}{c_w}$, K_n can be written as

$$K_n = \sqrt{\left(\frac{\omega}{c_w}\right)^2 - \left(\frac{n\pi}{H_e}\right)^2} \quad (23)$$

Furthermore, the group velocity of the n^{th} mode is given by

$$u_n = \frac{d\omega}{dK_n}, \quad (24)$$

therefore,

$$\begin{aligned} u_n &= \frac{c_w^2}{\omega} \sqrt{\left(\frac{\omega}{c_w}\right)^2 - \left(\frac{n\pi}{H_e}\right)^2} \\ &= c_w \sqrt{1 - \left(\frac{n\pi c_w}{\omega H_e}\right)^2} \end{aligned} \quad (25)$$

The group velocity u_n and the mode travel times are related by

$$t_n = \frac{R}{u_n}, \quad (26)$$

where R is the horizontal distance between source and receiver and t_n is the travel time of the n^{th} mode. Combining Eqs. (25) in (26) the mode travel times can be written

$$t_n = \frac{R}{u_n} = \frac{R}{c_w} \frac{1}{\sqrt{1 - \left(\frac{nc_w}{2fH_e}\right)^2}} \quad (27)$$

From the definition of effective depth, this becomes

$$t_n(f) = \frac{R}{c_w} \left\{ 1 - \left[\frac{n\pi \sin \theta_c}{\left(\frac{2\pi f H \sin \theta_c}{c_w} \right) + g} \right]^2 \right\}^{-1/2}, \quad (28)$$

which is the final expression for the mode travel times. Since we know the real depth H , and c_w and θ_c were determined from the previous analysis, then we can invert for g by

measuring the mode travel times over a range of frequencies for different SUS transmissions. Assuming $\rho_w \approx 1$, then $g \approx \rho_b$.

C. INVERSION OF BOTTOM ATTENUATION

Mode attenuation as a function of range can be estimated from several computed SUS spectrograms. The mode attenuation per km, α_n , satisfies the relation

$$\Delta TL_n = \alpha_n \Delta R, \quad (29)$$

where ΔTL_n and ΔR are the mode transmission loss due to attenuation and range between SUS drops, respectively. Neglecting volume attenuation in the water column, the decrease in mode amplitude is expected to be caused only by bottom attenuation and cylindrical spreading ($TL_{\text{spread}} = 10 \log R$). Since mode n can be thought of as due to rays propagating at angle θ_n , the mode attenuation can be considered the result of multiple bottom reflection losses.

The number of bottom bounces over 1 km of horizontal propagation can be found by considering the angle of elevation or depression θ of the local direction of propagation of the waveform. Referring to Figure 6, the angle θ and the diagonal distance for one bounce L_1 are related by

$$\sin \theta = \frac{2H}{L_1}, \quad (30)$$

where H is the water depth. Defining the total diagonal distance L corresponding to $R = 1$ km of horizontal propagation by

$$L = \frac{R}{\cos \theta}, \quad (31)$$

then L and L_1 can be related in order to define the number of bottom bounces per km as

$$N = \frac{L}{L_1} = \frac{R \tan \theta}{2H}. \quad (32)$$

The attenuation for mode n can then be expected to be due to $N(\theta_n)$ bottom bounces per km producing

$$\alpha_n = N(\theta_n) \alpha_{bb}(\theta_n), \quad (33)$$

where θ_n is the corresponding propagation angle for mode n and $\alpha_{bb}(\theta_n)$ is the bottom loss per bounce for a single reflection at this angle.

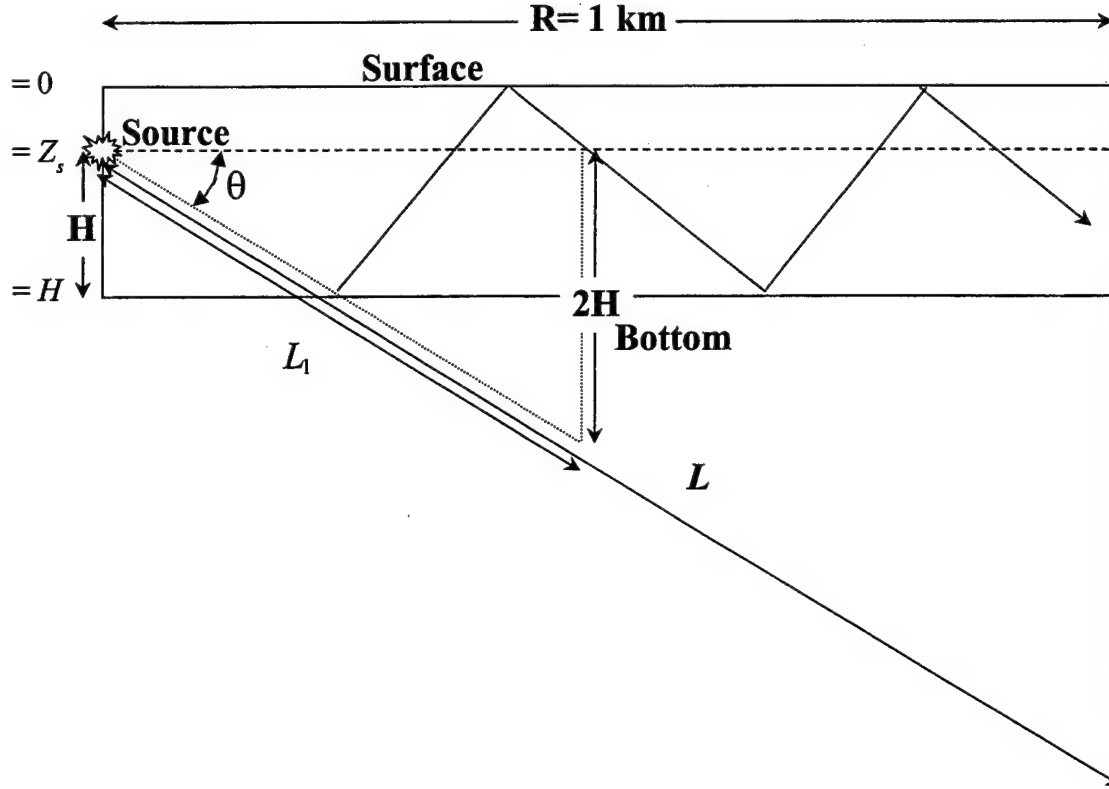


Figure 6. Geometry Used to Find the Number of Bottom Bounces.

The reflection coefficient at a fluid-fluid interface for a plane wave traveling at angle θ is defined by

$$R = \frac{\rho_b c_b \sin \theta + i \rho_w b_2}{\rho_b c_b \sin \theta - i \rho_w b_2}, \quad (34)$$

where c_w and ρ_w are the sound speed and density, respectively, in the upper medium, c_b and ρ_b are the sound speed and density, respectively, in the lower medium, and

$$b_2 = \left[\left(\frac{c_b}{c_w} \right)^2 \cos^2 \theta - 1 \right]^{1/2}. \quad (35)$$

If there is no attenuation, then $|R| = 1$ for incidence beyond the critical angle. However, if the bottom is lossy then

$$|R(\theta)| = 1 - \varepsilon(\theta), \quad (36)$$

and the bottom loss per bounce can be defined as

$$\alpha_{bb}(\theta_n) = -20 \log(|R(\theta_n)|) \cong 20\varepsilon(\theta_n). \quad (37)$$

Combining the equations above, the reduction in the reflection coefficient amplitude can be determined by

$$\varepsilon(\theta_n) = \frac{1}{20} \frac{\alpha_n}{N(\theta_n)} = \frac{1}{20} \frac{\Delta TL_n}{\Delta R N(\theta_n)}. \quad (38)$$

Bottom attenuation can be introduced by defining an imaginary component of the bottom sound speed,

$$c_b \rightarrow c_b - i\delta, \quad (39)$$

such that the wavenumber in the lower medium becomes

$$k_b = \frac{\omega}{c_b} \rightarrow k_b + i\alpha_e, \quad (40)$$

where

$$\alpha_e = \frac{\omega\delta}{c_b^2}. \quad (41)$$

Since the solution in the lower medium goes like

$$e^{ik_b R} \rightarrow e^{ik_b R} e^{-\alpha_e R}, \quad (42)$$

then α_e is found to produce the exponential decay in range. This then causes transmission loss according to

$$\Delta TL_{atten} = 8.686\alpha_e \Delta R = \alpha \Delta R, \quad (43)$$

where α is the bottom attenuation in units dB/m, and can be written as

$$\alpha = 8.686 \frac{\omega\delta}{c_b^2}. \quad (44)$$

In order to estimate the bottom attenuation (dB/m), a simple matching algorithm may be employed which searches over values of δ (the complex bottom sound speed) until

the reduction in the reflection coefficient amplitude agrees with the observed value of $\epsilon(\theta_n)$ defined in Eq. 37. Once values for δ are obtained (for various frequencies and mode angles θ_n), then Eq. 43 may be employed to produce the final estimate for the bottom attenuation α .

IV. DATA ANALYSIS AND RESULTS

A. INVERSION OF BOTTOM SOUND SPEED

As described in Section III. A., the inversion for bottom sound speed is based on the evaluation of the vertical coherence of the ambient noise field. For this analysis, the ambient noise was extracted from segments of the SUS data sets between actual SUS signals (and allowing for reverberation to fade). The spectrum of the ambient noise computed showed little variation from low frequency up to 600 Hz indicating no strong unexpected noise sources were present. Also, the imaginary component of the coherence between the two hydrophones was found to be small as required. This indicates that the ambient noise field at the trial site for frequencies below 600 Hz has a symmetrical distribution in the vertical direction and the data is suitable for inversion by the method described previously.

It should be noted that the inversion method described in Section III. A. was originally defined for an isospeed water column overlying a homogenous bottom. As is obvious from the local sound speed data (refer to Figure 2), there is significant variation in sound speed over depth. However, if the sound speed change is not too large over the vertical separation of the phones, the inversion method should still be applicable by simply adjusting the local angles to the appropriate values at the bottom interface using Snell's law.

Since the data from the upper two phones of the VLA was analyzed, a local sound speed of $c_w \approx 1485$ m/s was used in the calculation of the ambiguity function (refer to Eq. 11).

The fit between the theoretical coherence obtained from the model and the real component of the observed coherence is shown in Figure 7. By computing the ambiguity surface for the optimization of two parameters (a_2 and θ_c) an optimal value was found at $\theta_c \approx 18^\circ$ in the water column. Figure 8 shows the ambiguity surface for the optimization with two parameters, a_2 and θ_c whose minimum corresponds to $a_2 \approx 0.18$ and mean critical

angle $\theta_c \approx 18^\circ \pm 1^\circ$ for 4 different SUS explosive data. A grazing critical angle of approximately $19^\circ \pm 1^\circ$ near the bottom was determined from Snell's law. The sound speed close to the bottom was 1476 m/s, and therefore the bottom sound speed $c_2 \approx 1563 \pm 10$ m/s. This value was compared to values obtained by a sophisticated genetic algorithm technique employed at the University of Rhode Island (Miller and Potty, 1998). They found values in the upper few meters of the sediment in agreement with the result reported here.

B. INVERSION OF BOTTOM DENSITY

To invert for bottom density, the method of ideal waveguide effective depth was introduced. However, this method assumed a constant sound speed in the water column. In fact, this was fundamental in the definition of the ideal waveguide eigenfunctions. For that reason, this method may not be expected to produce very good results. We will attempt to invert for density anyway by assuming the water column is isospeed with nominal sound speed $c_w \approx 1485$ m/s. Consistent with this value, we shall assume the critical angle $\theta_c \approx 18^\circ$. In order to obtain separated mode travel times, spectrograms were computed for various SUS explosive data. The theoretical mode travel times, for the ideal waveguide were then computed as a function of range R between source (SUS) and receiver (VLA), water depth H , water sound speed c_w and critical angle θ_c . A comparison between theoretical and measured travel times for all 11 SUS data sets produced an average value for the density ratio of 1.6. However, the changes in the theoretical curves for various density ratios was not large whereas the mode arrival structures were fairly ambiguous. Thus the uncertainty is very large. It is also possible that the theoretical mode travel times have significant errors due to the mismatch in sound speed profile. However, the estimated value of $\rho_b \approx 1.6$ g/cm³ from the inversion method seems quite realistic. The results supplied by Miller and Potty suggest a more reasonable estimate for the bottom density is about 1.8 g/cm³. Figures 9a and 9b show the mode travel times for a phone from a SUS explosive data and those for an ideal waveguide.

C. INVERSION OF BOTTOM ATTENUATION

A method was developed in Section III.C. to invert for bottom attenuation using measures of modal transmission loss as a function of range. In order for this method to work successfully, the decrease in amplitude due to bottom attenuation must be observable over the transmission loss due to cylindrical spreading. For example, as the range between the SUS drop location and the VLA increases from 15 km to 30 km, the change in TL due to cylindrical spreading is approximately 3 dB. This equates to about 0.2 dB/km. In order for bottom attenuation to be distinguishable, Eq. (38) suggests that the quantity $20N \epsilon$ should be of this same order of magnitude or larger.

A simple analysis assuming bottom attenuation increase linearly with frequency shows that ϵ increases with increasing frequency. Specific values can be obtained using Eqs. (34) - (44) with realistic values of bottom attenuation α . However, as frequency increases, the angle of propagation for a specific mode decreases thereby decreasing N , the number of bottom interactions per km.

If one assumes a reasonable value of $\alpha \sim 0.05$ dB/km/Hz, a 100 Hz signal suffers a 0.5 dB/km loss due to attenuation for angles of propagation of about 12° . At this frequency in this waveguide, that corresponds roughly to Mode 2. Unfortunately, this mode is not clearly distinguishable at this frequency from the available SUS data. The lowest modes can be isolated at lower frequencies, but then the attenuation is negligible. At higher frequencies, the propagation angles for these low modes is near grazing, and again the influence of attenuation is small.

The result of this analysis, unfortunately, shows that this data does not avail itself to inversion for bottom attenuation using the method developed previously. Other processing methods may be able to extract the necessary information in order to utilize this method, but will not be explored further here.

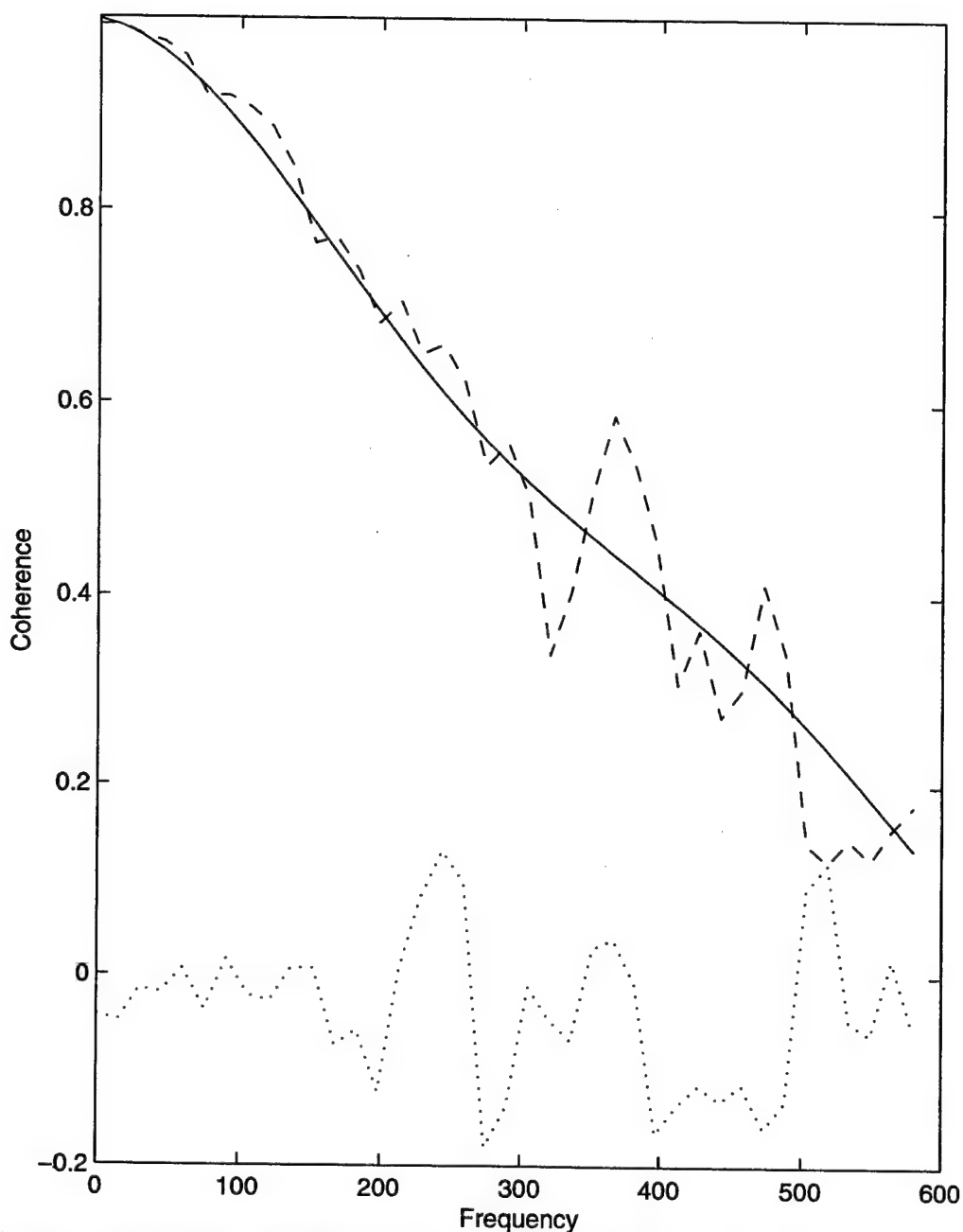


Figure 7. Coherence of the Measured Ambient Noise between Two Hydrophones; Real Component (Dashed Curve) and Imaginary Component (Dotted Curve). A Good Fit Between the Theoretical Coherence Obtained from the Model (Solid Line) and the Real of the Measured Coherence is Observed.

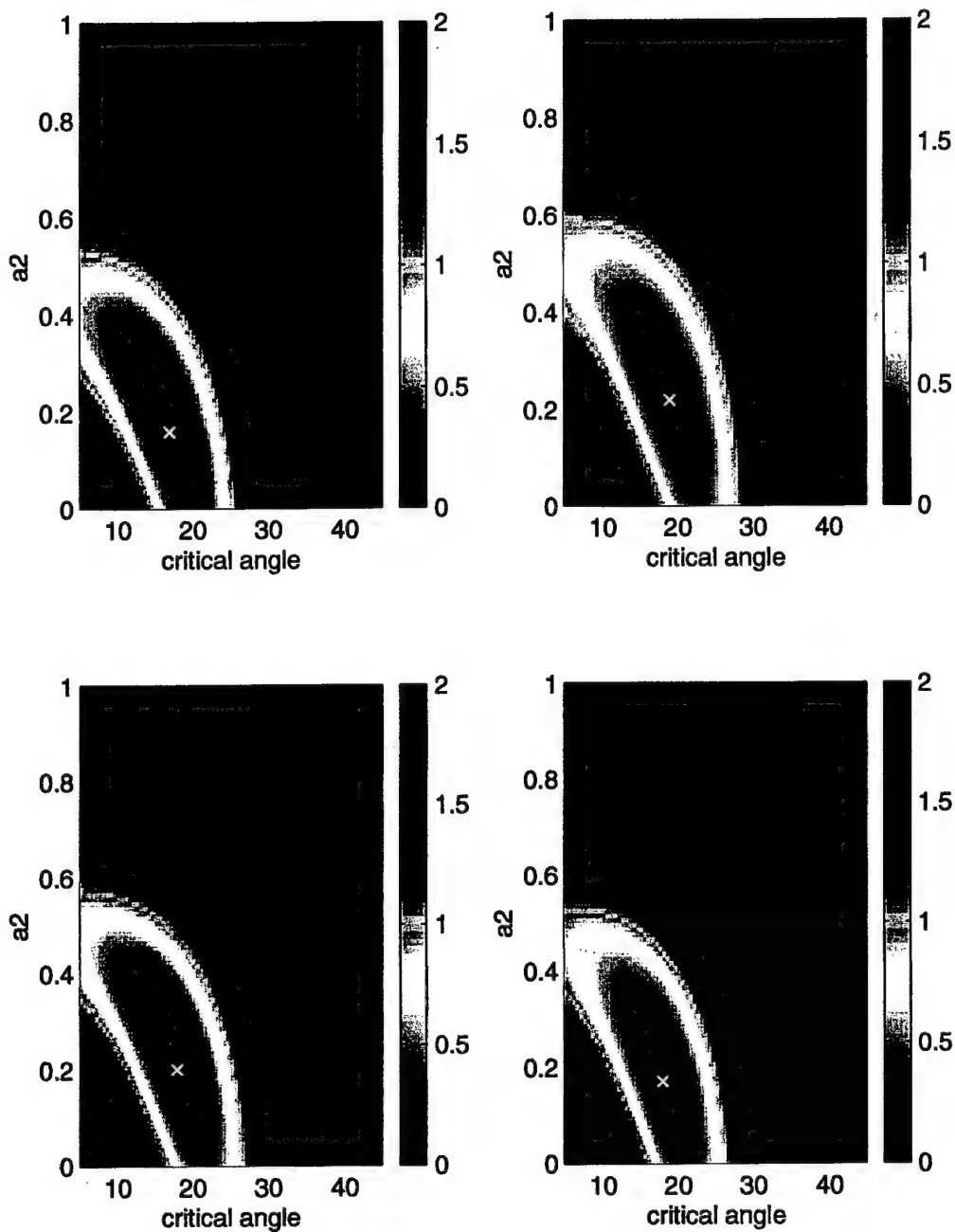


Figure 8. Ambiguity Surface for the Optimization with Two Parameters, a_2 and θ_c . The Minimum is Marked by X which Corresponds to $a_2 \approx 0.18$ and $\theta_c \approx 18^\circ$ for 4 Different SUS Explosive Data.

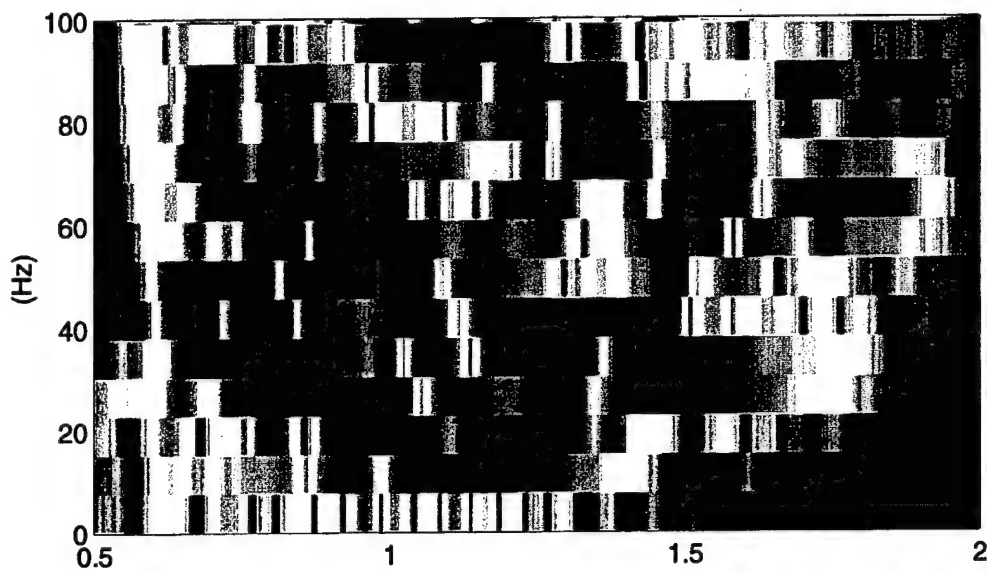


Figure 9a. Mode Travel Times for a Phone from a SUS Explosive Data.

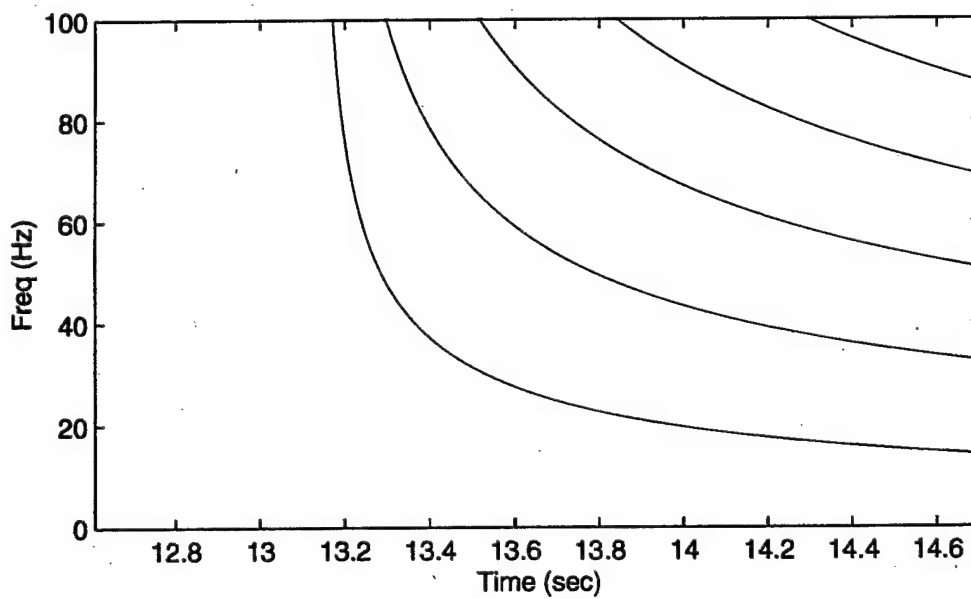


Figure 9b. Mode Travel Times for a Phone from an Ideal Waveguide.

V. CONCLUSION

This thesis incorporated several methods which may be applied directly to measured data to provide a relatively simple means of obtaining reasonable estimates of ocean bottom parameters from minimal information. The analysis of the data from the Mid-Atlantic Bight experiment recorded on the NW VLA produced the following results:

1. Ambient noise was used to measure both the vertical directionality and spatial coherence of the noise field. By examining the noise data, we have been able to estimate θ_c and hence the sound speed c_b in the sediment. The bottom sound speed deduced was approximately 1563 ± 10 m/s.
2. The method of effective depth was employed to estimate the bottom density ρ_b . Although this method was derived for an isospeed water column environment, it is expected to produce reasonable estimates for most shallow water environments. By comparing mode travel times extracted from SUS data spectrograms and comparing these with values for an ideal waveguide with an effective depth, the bottom density was estimated to be $\rho_b \approx 1.6$ g/cm³. The uncertainty in this value is very large, however, partly due to the difficulty in distinguishing mode arrivals clearly in the spectrograms.
3. In order to distinguish bottom attenuation from simple cylindrical spreading, it was determined that values for mode transmission loss were required for high modes at high frequencies. Unfortunately, the SUS spectrogram data could not adequately provide this information, and no estimate of bottom attenuation was produced. It may be possible to use the method outlined if a modal decomposition of the data on the VLA could be performed. However, due to the relatively short aperture of the array (compared to the waveguide depth), this seems unlikely. Furthermore, the source level of different SUS detonations may not be repeatable enough to use this data for accurate estimations of bottom attenuation.

Comparing the inversion results for bottom sound speed and density with values obtained from genetic algorithm techniques provided by the University of Rhode Island, good agreement was found particularly for the sound speed. However, the analysis of the SUS data proved more difficult than originally anticipated. Much of this has to do with the uncertainty in absolute drop location and repeatable source signals. Another part of the problem was the reliance on low mode information which is difficult to characterize for SUS data measured on only eight hydrophones with total aperture less than half the width of the waveguide. It is likely that this analysis would be more successful with different more well-defined sources and a full water column array.

LIST OF REFERENCES

- Buckingham, Michael J., and Stephen A. S. Jones, "A New Shallow-Ocean Technique for Determining the Critical Angle of the Seabed from the Vertical Directionality of the Ambient Noise in the Water Column," *J. Acoust. Soc. Am.*, 81 (4), April 1987.
- Chapman, David M. F., and Peter D. Ward, "The Effective Depth of a Pekeris Ocean Waveguide, Including Shear Wave Effects," *J. Acoust. Soc. Am.*, 85 (2), February 1989.
- Gawarkiewicz, Glen, Robert Pickart, James F. Lynch, Ching-Sang Chiu, Kevin Smith, and James Miller, "The Shelfbreak Front PRIMER Experiment," *J. Acoust. Soc. Am.*, 101 (5), May 1997.
- Jensen, Finn, B., William A. Kuperman, Michael B. Porter, and Henrik Schmidt, *Computational Ocean Acoustics*, p. 566, New York: American Institute of Physics, 1994.
- Kinsler, Lawrence E., Austin R. Frey, Alan B. Coppers, and James V. Sanders, *Fundamentals of Acoustics*, Third Edition, New York: John Wiley & Sons, 1982.
- Lynch, J. F., G. G. Gawarkiewicz, C. S. Chiu, R. Pickard, J. H. Miller, K. B. Smith, A. Robinson, K. Brink, R. Beardsley, B. Sperry, and G. Potty, "Shelfbreak PRIMER - An Integrated Acoustic and Oceanographic Field Study in the Middle Atlantic Bight," Proceedings of International Conference on Shallow Water Acoustics, Beijing, China, April 21-25, 1997. (Invited paper, in press.)
- Medwin, Herman and Clarence S. Clay, *Fundamentals of Acoustical Oceanography*, New San Diego, California: Academic Press, 1998.
- Miller, James H. and Gopu Potty, Personal Communication, University of Rhode Island, 1998.
- Pickart, Robert S., Glen G. Gawarkiewicz, James F. Lynch, Ching-Sang Chiu, Kevin Smith, and James H. Miller, "Endeavor 286 Cruise Summary: Primer III," 1996.
- Urick, Robert J., *Principles of Underwater Sound*, Second Edition, New York: McGraw-Hill, 1975.
- Weston, D. E., "A Moire Fringe Analog of Sound Propagation in Shallow Water," *J. Acoustic Soc. Am.*, 32, pp. 647-654, 1960.

INITIAL DISTRIBUTION LIST

	No. Copies
1. Defense Technical Information Center2 8725 John J. Kingman Rd., STE 0944 Ft. Belvoir, VA 22060-6218	
2. Dudley Knox Library2 Naval Postgraduate School 411 Dyer Rd. Monterey, CA 93943-5101	
3. Chairman, Code PH/Sk1 Engineering Acoustics Academic Committee Naval Postgraduate School Monterey, CA 93943-5101	
4. Professor Kevin B. Smith, Code PH/Sk4 Department of Physics Naval Postgraduate School Monterey, CA 93943-5101	
5. Professor Ching-Sang Chiu, Code OC/Ci1 Department of Oceanography Naval Postgraduate School Monterey, California 93943-5101	
6. Commander José G. Rojas1 599B Michelson St. Monterey, California 93940	
7. Dr. James F. Lynch1 Department of Applied Ocean Physics and Engineering Woods Hole Oceanographic Institution Woods Hole, Massachusetts 02543	
8. Dr. Jeff Simmen1 Office of Naval Research 800 North Quincy Street Arlington, Virginia 22217-5660	

9. Dr. Ellen Livingston1
Office of Naval Research
800 North Quincy Street
Arlington, Virginia 22217-5660
10. Professor James H. Miller.....1
Department of Ocean Engineering
University of Rhode Island
211 Sheets Building
Narragansett, RI 02882-1197